Nucleic Acids Research, 1994, Vol. 22, No. 15 3113–3118

Cooperative interaction of human HSF1 heat shock transcription factor with promoter DNA

Ying Wang and William D.Morgan*
Department of Biology and Centre for Human Genetics, McGill University, Montreal, Quebec, H3A 1B1, Canada

Received April 18, 1994; Revised and Accepted July 4, 1994

ABSTRACT

We investigated the thermodynamics and kinetics of binding of human HSF1 heat shock transcription factor to different configurations of heat shock element (HSE) sequences on DNA fragments, in order to analyze binding cooperativity under various conditions and to evaluate the significance of interactions between multiple HSE sites. Constructs with different arrangements of one or more copies of a 15 base pair idealized HSE sequence (AGAACGTTCTAGAAC) were used for *in vitro* binding experiments performed by multiple probe band shift assays and titrations. Dissociation kinetics under various conditions were also measured by band shift assays. These experiments indicated significant differences in behavior between constructs with a pair of tandem sites in correct orientation (forming a continuous array of alternating GAA and TTC blocks), and those with only a single site, or a pair of sites in reversed orientation. These differences in behavior indicated significant effects of cooperative binding to tandem sites *in vitro*, and showed in particular a strong temperature dependence of binding to different constructs. Thermodynamic parameters for binding affinity and cooperativity were also evaluated from direct titrations.

INTRODUCTION

The main goal of this study was to analyze cooperativity of binding by human heat shock transcription factor (HSF1) to arrays of multiple recognition sites. HSF is a highly conserved DNA-binding protein, found in many if not all eukaryotic organisms, that mediates the heat shock or cellular stress response. This response is a very convenient system for study of eukaryotic gene expression regulation and is also of considerable importance in physiology and medicine. The heat-inducible transcription of the stress proteins in human cells is controlled through the HSF1 factor, the product of one of several HSF-related genes (1). It has previously been shown that HSF from yeasts and *Drosophila* recognizes a 5 bp sequence motif, NGAAN and its complement, and that the basic mode of binding is an HSF trimer interacting with three adjacent 5 bp motifs (in alternating orientation). Thus, the basic form of a single binding element is the 15 bp sequence, NGAANNTTCNNGAAN (2–5). Strong response elements in these organisms appear to depend on the presence of multiple copies, suggesting that cooperative binding may contribute significantly to transcriptional activity, and cooperative binding of *Drosophila* HSF has been described (6).

Our previous studies of protein–DNA contacts showed that human HSF (from heat-shocked HeLa cells) also interacts with 5 bp DNA motifs by a very similar recognition mode. Extended arrays of tandem NGAAN motifs, created by site-directed mutagenesis of the heat-inducible human *HSP70.1* gene promoter, showed enhanced HSF binding *in vitro* and modestly improved *in vivo* expression (7). The recognition of the 5 bp motif has been analyzed in depth by saturation mutagenesis of this promoter, and the results established thermodynamic parameters to predict HSF binding affinity for variant sequence motifs, and corresponding levels of *in vivo* heat-inducible expression (8). In order to extend these studies, we wished to perform a quantitative analysis of binding cooperativity to tandem sites of two or more HSF trimer binding sites (i.e., 6 or more 5 base pair motifs). The blocks created in the context of the *HSP70.1* promoter, in previous work, varied in the actual sequence. In order to eliminate this variable, we created artificial arrays containing repeats of an identical 5 bp motif. The idealized consensus, AGAAC, whose sequence was derived from results of the previous saturation mutagenesis experiments, was used for this purpose. Different configurations with arrays of single or multiple repeats were thus created, and their thermodynamic and kinetic binding properties to human HSF1 were studied by a variety of methods.

MATERIALS AND METHODS

HSF1 protein expression

The human HSF1 coding sequence was derived from a 2.0 kilobasepair *Xho*I–*Bgl*II fragment that contained the coding region and 3′-nontranslated sequences (9). This fragment was cloned at the *Xho*I site of pGEX-KG, a derivative of the glutathione-S-transferase (GST) fusion protein vector pGEX-2T that has a modified polylinker sequence (10). The complete HSF1 cDNA, starting with the Met codon, was therefore placed in the correct reading frame downstream of the Arg-Gly thrombin

*To whom correspondence should be addressed at: Laboratory of Molecular Structure, National Institute for Medical Research, The Ridgeway, Mill Hill, London, NW7 1AA, UK

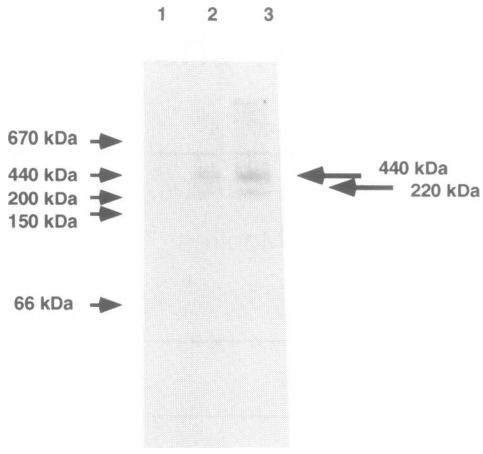

Figure 1. Pore exclusion limit gel electrophoresis of HSF1 oligomers. HSF1 expressed in *E.coli* was run for 24 h at 10 V/cm on a 4% to 20% polyacrylamide gradient gel and detected by Coomassie blue staining. Lane 1, 6 μg; lane 2, 12 μg; lane 3, 18 μg . Nondenaturing gel markers (Sigma) were: 670 kDa, thyroglobulin; 440 kDa, apoferritin; 200 kDa, beta-amylase; 150 kDa, alcohol dehydrogenase; 66 kDa, bovine serum albumin.

cleavage site. After cleavage, the protein contains a leader (GSPGISGGGGGILDSMGRLE) preceding the first codon of HSF1.

The pGEX-HSF1 constructs were expressed in *E.coli* JM109 by IPTG induction as described (10, 11), GST-HSF1 was recovered from the pellet by 4M guanidinium chloride extraction and stepwise dialysis into phosphate-buffered saline, bound to a glutathione-Sepharose column, eluted with thrombin, concentrated by membrane centrifugation into 20 mM Hepes (pH 7.0), 5 % glycerol, 0.1 mM EDTA, 1 mM DTT, 100 mM NaCl buffer (H(7.0) G5ED NaCl100), and stored in aliquots at −80°C. The total protein concentration (0.60 mg/ml) was determined by UV absorbance (12) and confirmed by Bradford assay. Purity was greater than 95% by densitometric analysis of Coomassie-stained polyacrylamide gels, with an apparent molecular weight of 72,000. The molar concentration of protein was calculated using a molecular weight of 58,000 predicted for the cDNA with the pGEX-KG leader sequence. The native size of the HSF1 oligomers was estimated by pore exclusion limit electrophoresis on 4 % : 20 % gradient gels in 0.5×TBE (13, 14). This experiment demonstrated the presence of two major species, with apparent relative molecular mass of 220,000 and 440,000 (Fig. 1). The proportion of the slower-migrating form is approximately 85% at the highest protein concentration. This band represents the major oligomeric species of HSF1 under these conditions, and although its migration is consistent with a hexameric form, other work (4) suggests that it may consist of a trimer with anomalous migration due to an extended conformation. The oligomeric state of HSF proteins may vary with experimental conditions. For example, fragments of the oligomerization domains of yeast HSF exist primarily as trimers at low salt, but aggregate into larger forms at higher salt conditions (≥ 100mM NaCl) (5).

Protein−DNA binding experiments

Multiple probe band shift assays were performed as described for binding of endogenous HeLa HSF to HSE probes (7, 8). The probes were restriction fragments of distinguishable length produced by digestion in the pUC118 polylinker. The 15, 30, and 45mer probes were labeled at the *Hin*dIII site and then cut with *Eco*RI; the 30-rev probe was labeled at the *Eco*RI site and then cut with *Pst*I. Reactions were incubated for 3 hr at the designated temperature in H(7.0) G5ED NaCl100 buffer with approximately 10^5 cpm of each probe, 1 μL of 10 A_{260} U/ml poly(dI-dC)·poly(dI-dC), and 0.6μg HSF1, in a volume of 15 μL. The eluted protein−DNA complexes and free probes were resolved by electrophoresis on denaturing polyacrylamide gels and quantified by densitometry. (7, 8, 15).

Dissociation rate analysis was performed as described (16). Reactions contained 4 fmol HSF1 and 0.1 nM DNA probe (8000 cpm) in a volume of 60 μL, in buffer conditions as described above for multiple probe assays. A 10 μL aliquot was loaded on the band shift assay gel at time zero, and 12 μL aliquots were loaded at the indicated time points subsequent to addition of 4 μg competitor HSE plasmid DNA (a synthetic 60mer with 12 tandem AGAAC and GTTCT repeats). The amount of bound complex was quantified by densitometry of autoradiographs, and for estimation of first order rate constants the data was fit to a single exponential decay equation using the Ultrafit program after background subtraction.

HSF1 titrations with the 30mer probe were performed by similar band shift assays in H(7.0) G5ED NaCl100 buffer, in a volume of 50 μL, incubated for 3 hr at the designated temperature, typically with 2.8 fmol of the DNA probe (0.056 nM total probe concentration). The fraction of probe in the bound complexes was quantified by densitometry.

Analysis of binding isotherms

The binding of the idealized $(AGAACGTTCTAGAAC)_2$ 30mer restriction fragment probe to HSF1 was considered in terms of a model previously described by Draper and von Hippel (17). This model is appropriate for binding of a ligand (protein) molecule to a small number of overlapping sites on an oligonucleotide. This model involves two thermodynamic binding parameters: the intrinsic association constant of a single ligand for its DNA binding site (K_{int}), and a cooperativity parameter, (y in the following description; omega in the original reference). The cooperativity parameter y expresses the interaction energy between two adjacent bound ligands , as defined by Hill (18):

$$y = \exp\{-\omega/kT\} \qquad \text{(Eq. 1)}$$

where omega is the interaction free energy between two adjacent bound ligand molecules. The treatment of Draper and von Hippel also involves two additional factors that are related to the number of ligand binding sites present on the oligonucleotide, and that serve as statistical factors to account for site overlap. These factors, S_1 and S_2, are defined as follows: S_1 is the number of individual binding sites available for the first ligand to bind to the oligonucleotide; S_2 is the number of sites available for potentially cooperative binding of a second ligand, when the first site is already occupied. $S_1 = (l - m + 1)$ where l is oligonucleotide length, and m is ligand binding site size; S_2 can be determined by inspection of the possible adjacent sites next to the first ligand at each position, according to a specific binding model. In the original treatment, where the ligand represents, for example, a protein binding nonspecifically to a site of several nucleotides or base pairs, l is the length in nucleotides (or basepairs). The model can be adapted to the present case of HSF−HSE interactions in the following manner: the length l is

the number of correctly oriented AGAAC repeats, and the site size m for HSF (considered as a trimer) is three. The formation of hexamers in the absence of DNA, and potential dissociation into monomers, are neglected. In the case shown for the 30mer probe (l=6), $S_1 = 4$, and $S_2 = 2$. Following the previous treatment, the apparent association constants K_1 and K_2 for binding of the first and second ligand are expressed as follows:

$$K_1 = S_1 K_{int} \quad \text{(Eq. 2)}$$

$$K_2 = (S_2/S_1) y K_{int} \quad \text{(Eq. 3)}$$

Furthermore, the extent of binding of the labeled restriction fragment probe (D), as a function of the protein concentration (P) can be represented by a binding polynomial:

$$[D_{bound}] = K_1[P][D_{free}] + K_1K_2[P]^2[D_{free}] \quad \text{(Eq. 4)}$$

It should be noted that the treatment below diverges from the original (17), since the experimental method used, the band shift assay, gives the fraction of probe bound (containing one or more protein molecules), rather than the binding density as such. The fraction of probe bound (with either one or two trimers, designated r, is then described by:

$$r = (4K_{int}[P] + 2yK_{int}^2[P]^2)/(1 + 4K_{int}[P] + 2yK_{int}^2[P]^2) \quad \text{(Eq. 5)}$$

This equation was used to fit the 30mer probe band shift assay data by nonlinear least-squares analysis with the UltraFit program (Biosoft). Since the protein was in molar excess, P_{total} is approximately equal to P_{free}, and total added protein concentration was used. Similar fits could be obtained with a range of values, by simultaneously adjusting the two parameter K_{int} and y. Therefore, for the final fits shown here, a constant value of K_{int} in the appropriate range was assumed, and the corresponding values of y at different temperatures were estimated by curve-fitting.

For an alternative estimate by another method, a plausible range for the value of y was obtained. This approach (19) was previously used to obtain an estimate for the extent of cooperativity in band shift assays, for a probe with two adjacent (nonoverlapping) sites. The maximum fraction (f_I max) of the probe present in the form of the singly bound species is determined, as protein concentration is varied. In the case of strong cooperativity, this value will be very low, whereas in the absence of cooperativity, the singly bound complex will be a major species at the midpoint of the titration. This general approach can be applied to the present case, although in contrast to the original model, binding site overlap should be considered. Using the statistical correction factors as in Draper and von Hippel, the apparent S_1 and S_2 described above, binding constants K_1 and K_2, and following the derivation of Tsai *et al.* (19), the expression for f_I max is:

$$y = 2\left(\frac{1}{f_I \text{max}} - 1\right)^2 \quad \text{(Eq. 6)}$$

where f_I is the fraction of the faster-migrating complex. Essentially, the overlapping sites mean that in the absence of cooperativity, a greater value of f_I max would be expected than in the nonoverlapping case. The above equation (Eq. 6) was used to calculate plausible limits for the value of y.

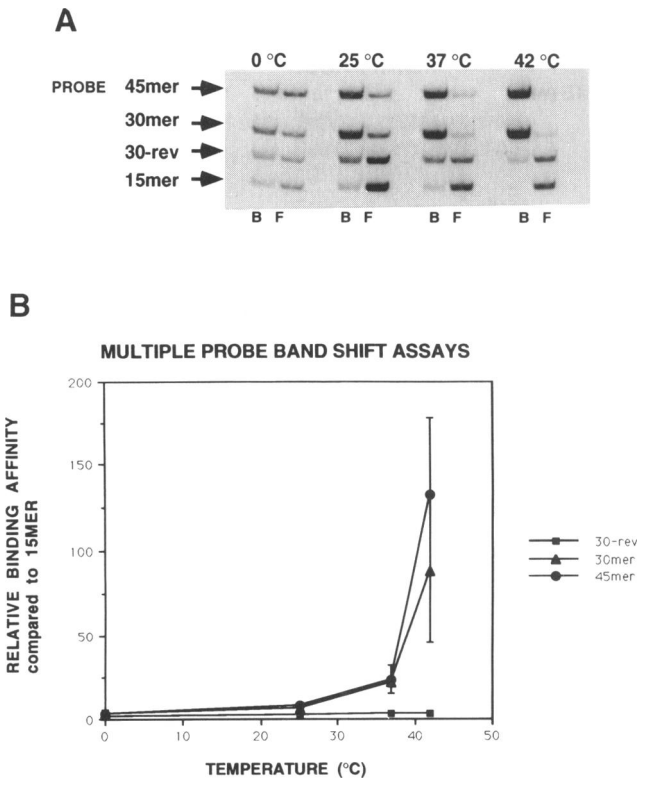

Figure 2. Multiple probe band shift assay with different configurations of HSE units. [**A**] Idealized HSE consensus probes consisted of (1) the basic 15mer, AGAACGTTCTAGAAC; (2) the 30mer with 6 5 bp motifs in alternating orientation, AGAACGTTCTAGAACGTTCTAGAACGTTCT; (4) the 30mer-rev also with 6 5 bp motifs, but with reversed orientation of three of the motifs, AGAACGTTCTAGAACAGAACGTTCTAGAAC; and (4) the 45mer sequence AGAACGTTCTAGAACGTTCTAGAACGTTCTTCTAGAACGTTCT. Probes created from the four constructs were simultaneously incubated at the indicated temperature in a volume of 40 μL with 0.7 fmol of HSF1 (trimers) at a concentration of 1 nM for each probe. Bound complexes and free probe were separated by preparative gel electrophoresis, electroeluted and run on subsequent denaturing gels to resolve the four different length probes. [**B**] Relative HSF1 binding to the different HSE arrays was quantified by densitometry. The relative distribution of bound and free probe in each case was used to calculate apparent relative affinities for the different constructs, as described previously (7, 8). The values were expressed for the 30mer, 30-rev, and 45mer probes relative to that for the 15mer probe.

RESULTS

Four different constructs were made by cloning a 15bp double-stranded consensus oligonucleotide (AGAACGTTCTAGAAC) into pUC vectors (Fig. 2A). The two 30 bp constructs differ in the internal orientation of the two 15 bp units. The 30mer construct has tandem repeats, in alternating orientation throughout. The other construct, 30-rev, has the second 15 bp site reversed relative to the first. The binding of HSF *in vitro* to these constructs was first examined directly by DNase I footprinting. Experiments with these constructs used human HSF1 cDNA expressed in *E.coli* as a glutathione-S-transferase fusion protein, purified by affinity chromatography and cleaved from the GST carrier. This experiment demonstrated that, as expected, a 20 bp footprint was observed with the 15mer construct, and protected regions increased in proportion to the number of motifs present , while weak binding to a 10 bp site was also observed (data not shown). The standard buffer for these

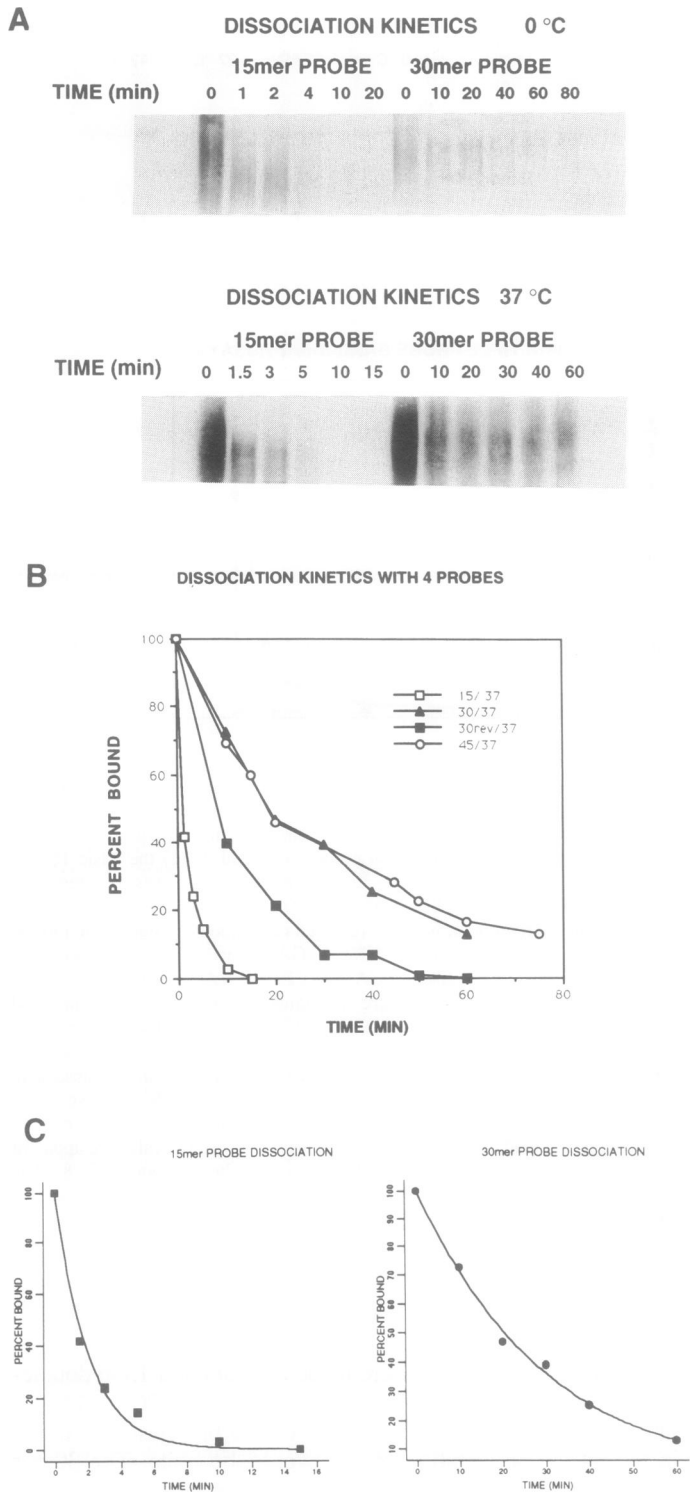

Figure 3. HSF complex dissociation kinetics. [A] Dissociation of HSF1–DNA complexes measured on band shift assay gels. Complexes were prepared by incubation of 4 fmol HSF1 with the indicated probe at 0.1 nM concentration at the temperature shown, and sample aliquots were loaded on gels at the time indicated after addition of 500-fold excess unlabeled competitor DNA (containing a 60 base pair element with tandem AGAAC and GTTCT motifs). The apparent migration of complexes changed since the gels were run continously as the successive aliquots were loaded. Only the bound complexes are shown. [B] Dissociation of HSF–DNA complexes at 37°C with various probes. Bound complexes and free probe bands from gels similar to that shown in Fig. 3A were quantified by densitometry. [C] Kinetic analysis: densitometric data from experiments as shown in Fig. 3A,B with the indicated probes at 37°C was fit with nonlinear least-squares analysis to a single exponential decay equation.

experiments was H(7.0)G5ED, 100mM NaCl (see Materials and Methods). In preliminary experiments, this buffer resulted in somewhat stronger binding than the corresponding pH 7.5 solution, or the previously employed Tris buffer (data not shown). In addition, some experiments were performed in standard buffer containing 5 mM $MgCl_2$, as described below.

Relative binding of these four idealized HSE constructs was first examined by multiple probe band shift assays and dissociation kinetics. The former procedure, as described previously (7, 8), determines the relative binding affinities of different probes, on band shift gels, from their pattern of distribution between the free and bound complex bands. This information can be used to calculate relative values of apparent association constants for the different HSE species. The values of apparent binding constants for the HSE constructs 30, 30-rev, and 45 are shown relative to the single binding site 15mer construct. These results (Fig. 2) showed that all of the multiple-site constructs had higher binding affinity than the 15mer, in the rank order 15 < 30-rev < 30 < 45. The difference was relatively small for 30-rev, approximately two-fold, and probably can be explained by the presence to two (almost completely) independent binding sites of similar affinity to the single site of the 15mer. The most striking feature, however, was the dramatic temperature dependence of relative binding affinity for the 30 and 45 constructs. These have only moderately stronger binding (3 to 4-fold), relative to the 15mer, at 0°C. In contrast, at 37°C and 42°C (normal growth and heat shock temperatures, respectively) the binding affinity for these constructs compared to the 15mer increases to 20-fold (37°C) and then to more than 100-fold (42°C). The 30-rev construct, on the other hand, showed no significant variation in relative binding compared to the 15mer, throughout this temperature range. These results strongly suggest that it is the presence of two tandem sites in correct alternating orientation (in the 30 and 45mers), rather than simply the number of 5 bp motifs or 15 bp binding sites, that is involved in the increased affinity at high temperature. Similar results were obtained with in standard buffer containing in addition 5 mM $MgCl_2$, except that relative affinity of the 30mer and 45mer, compared with the 15mer, was moderately (2 to 4-fold) improved. Thus, the presence of $MgCl_2$ may modestly enhance the effect of cooperative binding to tandem sites.

These four constructs were also investigated with respect to dissociation kinetics (Fig. 3). There are two trends evident from these results. First, there was a moderate decrease in dissociation rates (at all temperatures in the range from 0°C to 42°C), in the series 15mer > 30-rev > 30mer, 45mer. This generally corresponds to an increasing number of 5 bp motifs (although 30-rev probe had a higher dissociation rate than the 30mer). Second, the dissociation rates for each construct increased moderately with increasing temperature. This latter observation indicates that the temperature-dependent increase in affinity in multiple probe band shift assays, described above, for the 30mer and 45mer constructs, is not simply due to greater kinetic stability at high temperature. Furthermore, the multiple probe assays were incubated for 3 hr at the indicated temperature in order to reach equilibrium. Kinetic parameters were measured by further analysis of this data for the 15mer and 30mer probes at various temperatures. First-order dissociation rate constants for the 15mer and 30mer probes are shown in Table I.

Further experiments were performed with the 30mer probe in order to investigate binding isotherms, and to provide quantitative estimates of the intrinsic binding affinity and strength of

cooperative interactions. Band shift assays were performed at constant probe concentration, and at a range of HSF1 concentrations. Equilibrium binding experiments with the 30mer construct are shown in Fig. 4. The major band represents a pair of bound trimers (or a single hexamer) as indicated by footprinting experiments. A minor species that migrates slightly faster probably corresponds to a singly bound complex with one trimer, as seen with Drosophila HSF (20). The fraction bound (r in Eq. 5) was calculated by densitometry from the total of both bands. In practice, the minor band is not significant for these calculations, as it typically contained approximately 5% of the total. The increase in binding affinity at higher temperature was evident here also. Furthermore, the shape of the binding isotherm is sigmoidal, consistent with the existence of cooperative binding interactions. The binding isotherm can be accounted for according to one specific model, in terms of the intrinsic association constant for binding of a single HSF1 trimer to three tandem alternating 5 bp motifs (K_{int}) and a cooperativity parameter (y) representing interaction energy between two adjacent trimers bound to a pair of correctly oriented neighboring sites (see Materials and Methods). The equation derived from this model (Eq. 5) was used to estimate the value of these two parameters by a nonlinear least-squares fitting procedure. In practice, the best fit value of y was obtained for a given value of K_{int}. The curve obtained with values of 10^6 M^{-1} for K_{int}, and 247 (±58, 95% confidence interval) for y, (standard buffer, 37°C) is shown in Fig. 4B. It should be noted that these fits were made using the total HSF1 concentration for calculations, and will represent an underestimate of K_{int} if the fraction of protein active for DNA binding is less than 100%.

It is also possible to obtain a rough estimate of y from the maximum fraction of singly bound complex as a function of protein concentration (19). The greater the extent of binding cooperativity, the lower this maximum will be. Maximum values of 5% to 10% singly bound complex observed with the 30mer probe at 37°C indicated that a plausible range of values for y was 64 to 300. Similar analysis was performed at 0°C and at 42°C. (Fig. 4B) The values of y at these temperatures (± 95% confidence interval) were 52 ± 19 (0°C) and 233 ± 38 (42°C). The binding parameters at 42°C were indistinguishable within experimental error to those obtained at 37°C. Different

Table I. Summary of first-order kinetic rate constants for dissociation of various HSE constructs at different temperatures.

HSF1 complex dissociation constants		
	temperature (°C)	dissociation rate constant (min^{-1})
15mer probe		
	0	0.058 ± 0.007
	25	0.20 ± 0.09
	37	0.56 ± 0.15
	42	0.74 ± 0.40
30mer probe		
	0	0.013 ± 0.004
	25	0.021 ± 0.007
	37	0.035 ± 0.016
	42	0.069 ± 0.061

Kinetic constants were determined by plots similar to that shown in Fig. 3C. Error estimates represent 95% confidence intervals.

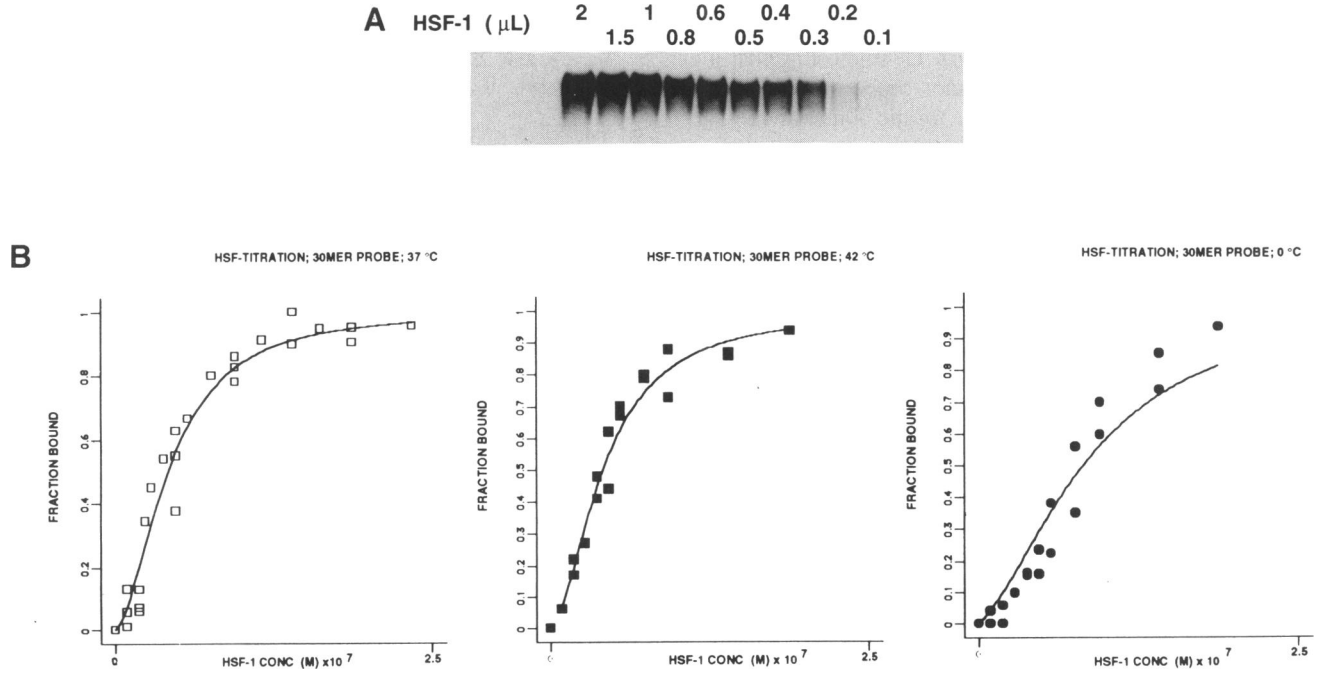

Figure 4. HSF1: 30mer probe band shift assay titrations. [A] The 30mer probe (2.8 fmol; 0.56 nM total concentration) was incubated for 3 h at 37°C with the volume of HSF1 (4 μM trimers) indicated for each lane in an assay volume of 50 μL, and then applied to a nondenaturing gel. Only the bound complexes are shown. [B] The percent bound probe at each temperature was quantified by densitometry of autoradiograms. The total bound probe (sum of major and minor bands; see text) was calculated . The concentration of HSF is given in terms of concentration of trimers (assuming all the protein is oligomerized). Binding curves were drawn by nonlinear least-squares analysis with the equations described in Materials and Methods. Open squares, 37°C; filled squares, 42°C; filled circles, 0°C.

parameters were obtained with this probe at 0°C, reflecting the much lower affinity under these conditions. This result suggested that either intrinsic affinity, or extent of cooperativity, or both, decreased at lower temperature. The quality of fit also decreased, indicating that the model described here may not apply at all conditions. One possible explanation for the poor fit is that the oligomerization state of the protein may be changing as a function of lower temperature (4).

DISCUSSION

The estimation of the thermodynamic parameter for cooperativity that describes the interaction of HSF1 with a tandem HSE should be very useful in explaining *in vivo* occupancy of HSE sites as a function of the concentration of activated HSF, and therefore complements previous work that analyzed in detail the dependence of intrinsic binding affinity on DNA sequence variation within mutant HSEs. Although these particular elements were not tested for heat-inducible transcription, previous work with extended arrays of 5 base pair motifs in HeLa cells indicates that they would almost certainly be very strong (7). This investigation also provided very interesting insights into the behavior of HSF1 in DNA–protein interactions. The measurement of the apparent binding affinity for a tandem double site, relative to a single 15bp HSE, revealed an unexpectedly strong effect of temperature on apparent cooperativity between adjacent sites. This is consistent with the previous qualitative observation that *Drosophila* HSF appeared to have a greater extent of cooperativity at 37°C than at lower temperature (6). The weaker binding observed in direct titrations with the 30mer probe at 0°C, compared to 37°C and 42°C, is consistent with the dramatic change in preference for the 30mer probe relative to the 15mer in multiple probe band shift assays. Interestingly, the direct titrations with the 30mer probe indicated similar binding affinity and cooperativity at 37°C and 42°C, suggesting that it may be a change in binding to the 15mer probe at 42°C that results in a further increase in preference for the 30mer at 42°C, as shown in Fig. 2A,B. Furthermore, although a previous study did not appear to exhibit strong cooperativity of *in vitro* binding (defined as the preference for a tandem site compared to a single one), those experiments were generally performed at 0°C. This is consistent with the observation that cooperativity between tandem sites is minimal at that temperature.

Observations in the present study have several implications for heat shock regulation *in vivo*. First, there may be a significant modulation of the degree of binding to tandem rather than isolated sites during a typical temperature shift of 37°C to 42°C for mammalian cells, affecting the distribution of HSF1 among different promoter sites. The reduced affinity and cooperativity of HSF1 binding at 0°C and 25°C may be relevant to events at abnormally low temperature. One current model for heat shock suggests that there is negative regulation of HSF by direct interaction with HSP70 molecules, and that induction involves relief of this effect when the cellular pool of free HSP70 is depleted by cell damage (1). The temperature dependence of HSF1 cooperative binding may mean that a given amount of damage and HSP70 depletion might have a smaller induction effect if it occurred below normal temperature.

There is a further possibility for involvement of cooperative interactions in the regulatory process. It has been proposed that, *in vivo*, attenuation of the heat shock response during recovery, which requires 5 to 10 min, proceeds much more rapidly than the rates of *in vitro* dissociation of HSF from strong promoter sites (typically containing extended arrays of 5 base pair motifs) (22). This suggests that attenuation may involve the facilitation of complex dissociation. The rate measurements in the present study are consistent with this, indicating that an extended 30 base pair site with motifs in the correct orientation may form complexes with a half life of 40 min or more at 37°C *in vitro*, although dissociation of complexes with isolated 15 base pair elements is approximately 10-fold faster. These observations suggest that dissociation from extended arrays or promoters with multiple sites might result from disruption of cooperative interactions between HSF trimers, followed by spontaneous dissociation of the isolated trimers at a faster rate. This process might also involve the action of hsp70 as a negative regulator, since it can interact with HSF1 and appears to be involved in the attenuation process, but does not prevent DNA binding by HSF trimers even when complexed with them (21). Disruption of cooperative interactions by HSP70 protein binding, consistent with its known ability to alter protein conformation, could create kinetically unstable isolated trimers and thus catalyze the attenuation process.

ACKNOWLEDGEMENT

We are grateful to C.Wu for providing the human HSF1 cDNA clone.

REFERENCES

1. Morimoto, R. I. (1993) *Science*, **259**, 1409–1410.
2. Sorger, P. K. (1991) *Cell* **65**, 363–366.
3. Lis, J. T., Xiao, H., and Perisic, O. (1990) in *Stress Proteins in Biology and Medicine* (Morimoto, R. I., Tissieres, A., and Georgopoulos, G., eds.) pp. 411–428, Cold Spring Harbor Laboratory, Cold Spring Harbor, NY.
4. Rabindran, S. K., Haroun, R. I., Clos, J., Wisniewski, J., and Wu, C. (1993) *Science*, **259**, 230–234.
5. Peteranderl, R., and Nelson, H. C. M. (1992) *Biochemistry*, **31**, 12272–12276.
6. Xiao, H., Perisic, O., and Lis, J. T. (1991) *Cell*, **64**, 585–593.
7. Cunniff, N. F. A., Wagner, J., and Morgan, W. D. (1991) *Mol. Cell. Biol.*, **11**, 3504–3514.
8. Cunniff, N. F. A., and Morgan, W. D. (1993) *J. Biol. Chem*, **268**, 8317–8324.
9. Rabindran, S. K., Giorgi, G., Clos, J., and Wu, C. (1991) *Proc. Nat. Acad. Sci. U. S. A.*, **88**, 6906–6910.
10. Guan, K., and Dixon, J. E. (1991) *Anal. Biochem.*, **192**, 262–267.
11. Waterman, M. L., Fischer, W. H., and Jones, K. A. (1991) *Genes and Devel.*, **5**, 656–669.
12. Gill, S. C., and von Hippel, P. H. (1989) *Anal. Biochem.*, **182**, 319–326.
13. Andersson, L. O., Borg, H., and Mikaelsson, M. (1972) *FEBS Lett.*, **20**, 199–201.
14. Clos, J., Westwood, J. T., Becker, P. B., Wilson, S., Lambert, K., and Wu, C. (1990) *Cell*, **63**, 1085–1097.
15. Gilman, M. Z., Wilson, R. N., and Weinberg, R. A. (1986) *Mol. Cell. Biol.*, **6**, 4305–4316.
16. Li, R., Knight, J., Bream, G., Stenlund, A., and Botchan, M. (1989) *Genes and Devel.*, **3**, 510–526.
17. Draper, D. E., and von Hippel, P. H. (1978) *J. Mol. Biol.*, **122**, 321–338.
18. Hill, T. L. (1985) *Cooperativity Theory in Biochemistry*, p. 169, Springer Verlag, NY.
19. Tsai, S. Y., Tsai, M.-J., and O'Malley, B. W. (1989) *Cell*, **57**, 443–448.
20. Perisic, O., Xiao, H., and Lis, J. T. (1989) *Cell*, **59**, 797–806.
21. Abravaya, K., Myers, M. P., Murphy, S. P., and Morimoto, R. I. (1992) *Genes and Devel.*, **6**, 1153–1164.
22. Abravaya, K., Phillips, B., and Morimoto, R. I. (1991) *Genes and Devel.*, **5**, 2117–2127.